EXPLICIT ORDER MODEL FOR REGION-BASED LEVEL SET SEGMENTATION

Lingfeng Wang and Chunhong Pan

NLPR, Institute of Automation, Chinese Academy of Sciences
{lfwang@nlpr.ia.ac.cn, chpan@nlpr.ia.ac.cn}

ABSTRACT

Region-based level set methods have been widely used for image segmentation. Among them, the method based on local binary fitting (LBF) model is an efficient one. Unfortunately, LBF model is sensitive to initial contour. To overcome this disadvantage, we propose two explicit order models, i.e., the global order preserving and local order smoothness models. The global order preserving model ensures that the binary fitting values have the same order globally, while the local order smoothness model requires that these orders are smooth locally. With these two models, our segmentation results are not sensitive to initializations. Experimental results on synthetic and real images show desirable performances of our method, as compared with the state-of-the-art approaches.

Index Terms— Image Segmentation, Level Set, Region-based, CV Model, LBF Model

1. INTRODUCTION

Medical image segmentation is an fundamental task in many image processing systems. However, it is still a challenging problem due to following practical difficulties, i.e., complex noise and intensity inhomogeneity. To tackle these difficulties, a number of methods have been proposed. Among them, level set based methods have proved to be a successful branch.

Level set based segmentation methods can be mainly divided into two groups, such as edge-based [1, 2, 3, 4, 5, 6] and region-based [7, 8, 9, 10, 11, 12, 13, 14, 15, 16]. Edge-based methods use edge information represented by image gradient to drive the active contours. Unfortunately, due to the calculation of image gradient, these methods are sensitive to noise. On the contrast, the region-based methods, which exploit the statistical information inside and outside the contour, are less sensitive to noise and weak edges.

1.1. CV and LBF Models

The classical region-based segmentation model, called CV model, is proposed by Chan *et al.* in [7]. Let $\Omega \subset \mathbb{R}^2$ be the two dimensional image domain, and $I : \Omega \to \mathbb{R}$ be the given gray-level image. CV model is proposed to minimize the following energy functional

$$\mathcal{F}_{cv}(\mathcal{C}, c^f, c^b) = \lambda_f \int_{\Omega_f} |I(\mathbf{x}) - c_f|^2 \, d\mathbf{x} + \lambda_b \int_{\Omega_b} |I(\mathbf{x}) - c_b|^2 \, d\mathbf{x} + \nu \text{Len}(\mathcal{C}), \quad (1)$$

where λ_f, λ_b and ν are three positive weighting constants. $\text{Len}(\mathcal{C})$ represents the length of segmentation contour $\mathcal{C}$. Ω_f and Ω_b are the foreground (or object) and background regions determined by the segmentation contour $\mathcal{C}$. Two parameters c_f and c_b are the clusters of foreground and background regions.

The core idea behind CV model is assuming that image intensities are statistically homogeneous in each segmented region. Therefore, the CV model cannot effectively tackle the intensity inhomogeneity problem. To overcome the drawback of CV model, Li *et al.* [12] proposed a local region-based segmentation model, called LBF model. In LBF model, a local energy is first constructed in each local region due to a kernel function, given by

$$\mathcal{F}_{local}(\mathcal{C}, C_f(\mathbf{x}), C_b(\mathbf{x})) = \lambda_f \int_{\Omega_f} K_{\sigma,\mathbf{x}}(\mathbf{y}) \, |I(\mathbf{y}) - C_f(\mathbf{x})|^2 \, d\mathbf{y} + \lambda_b \int_{\Omega_b} K_{\sigma,\mathbf{x}}(\mathbf{y}) \, |I(\mathbf{y}) - C_b(\mathbf{x})|^2 \, d\mathbf{y}, \quad (2)$$

where

$$K_{\sigma,\mathbf{x}}(\mathbf{y}) = \frac{1}{2\pi\sigma^2} \exp\left\{\frac{-\|\mathbf{x}-\mathbf{y}\|^2}{2\sigma^2}\right\}$$

is the Gaussian kernel function parameterized with the scale parameter σ. $C_f(\mathbf{x})$ and $C_b(\mathbf{x})$ can be regarded as the local foreground and background clusters at location $\mathbf{x}$. Then, the total energy is defined based on the integration of the whole image domain:

$$\mathcal{F}_{lbf}(\mathcal{C}, C_f, C_b) = \int_{\Omega} \mathcal{F}_{local}(\mathcal{C}, C_f(\mathbf{x}), C_b(\mathbf{x}))d\mathbf{x} + \nu \text{Len}(\mathcal{C}). \quad (3)$$

As reported in [12], LBF model can solve intensity inhomogeneous well. However, as discussed in [15] and [16], LBF model is sensitive to the initial contours. The main reason is that LBF model does not restrict the local clusters (or fitting values) C_f and C_b.

1.2. The Proposed Method

Motivated by previous work, in this paper, we propose two explicit order models by constraining the local clusters so as to remedy the initialization sensitive problem of the LBF model. The details or main advantages of our method are summarized as follows:

- We propose two explicit order models, i.e., the global order preserving (GOP) and local order smoothness (LOS) models. Based on GOP and LOS models, our segmentation method is less sensitive to initializations than the LBF [12].
- A new semi-implicit optimization method is proposed to solve the objective functional, in which local clusters C_f and C_b are obtained iteratively.

The remainder of this paper is organized as follows: Section 2 introduces the proposed implicit order models in detail. In Section 3, we present our segmentation method. Experiments results are given in Section 4. The concluding remarks are discussed in Section 5.

This work was supported in part by the National Natural Science Foundation of China (Grant Nos. 61403376, 61175025 and 61370039).

2. IMPLICIT ORDER MODEL

For each pixel located at $\mathbf{x} \in \Omega$, the local foreground and background clusters are $C_f(\mathbf{x})$ and $C_b(\mathbf{x})$, respectively. The order of local clusters is defined as

$$O(\mathbf{x}) = H(C_f(\mathbf{x}) - C_b(\mathbf{x})), \tag{4}$$

where $H(.)$ is the Heaviside function.

2.1. Global Order Preserving Model

The purpose of segmentation is to divide an input image into two segments, i.e., object and background. In most image, the object is brighter (or darker) than background within a local region, and this brighter (or darker) relationship can be preserved globally in a whole image domain. Here, we only consider the case that the object is brighter than background. In such case, in a local region centered at $\mathbf{x}$, the two fitting value $C_f(\mathbf{x})$ and $C_b(\mathbf{x})$ should satisfy the following condition: $C_b(\mathbf{x}) < C_f(\mathbf{x})$. To preserve this property, we propose a new GOP energy, given by

$$\mathcal{F}_{op}(C_f, C_b) = \int w(\mathbf{x}) O(\mathbf{x})^2 d\mathbf{x}, \tag{5}$$

where $w(\mathbf{x})$ is a weighting value calculated by

$$\begin{aligned} w(\mathbf{x}) &= \int B(\mathbf{x}, \mathbf{y}) d\mathbf{y} \\ &= \int \exp\left(-\frac{(I(\mathbf{x}) - I(\mathbf{y}))^2}{2\sigma_c^2}\right) \cdot \frac{1}{\|\mathbf{x} - \mathbf{y}\|_2} d\mathbf{y}, \end{aligned} \tag{6}$$

where σ_c is the standard deviation of intensity. The purpose of using weighting value is to strengthen smooth regions while weakening edges.

2.2. Local Order Smoothness Model

As mentioned above, GOP model is proposed to ensure that object should be brighter (or darker) than background. However, if there are two objects, one is brighter than background while the other is darker, the segmentation algorithm with only GOP energy will fail to segment two objects simultaneously. To solve this problem, we propose a new local order smoothness (LOS) model

$$\mathcal{F}_{os}(C_f, C_b) = \int \mathcal{F}_{los}(\mathbf{x})^2 d\mathbf{x}, \tag{7}$$

where $\mathcal{F}_{los}(\mathbf{x})$ is local order smoothness function center at point $\mathbf{x}$, which is defined as follows

$$\mathcal{F}_{los}(\mathbf{x}) = \int B(\mathbf{x}, \mathbf{y})(O(\mathbf{x}) - O(\mathbf{y}))^2 d\mathbf{y}. \tag{8}$$

From Eqns. (7) and (8), we see that LOS model ensures that two pixels should have equal order if they are nearby and similar in intensity (refer to [17] for more information).

3. THE PROPOSED SEGMENTATION METHOD

By incorporating GOP and LOS models into the original LBF model, we can obtain the objective functional of our segmentation method based on explicit order (EO) model:

$$\begin{aligned} \mathcal{F}_{eo}(\mathcal{C}, C_f, C_b) = \mathcal{F}_{lbf}(\mathcal{C}, C_f, C_b) \\ + \eta_1 \mathcal{F}_{op}(C_f, C_b) + \eta_2 \mathcal{F}_{os}(C_f, C_b), \end{aligned} \tag{9}$$

where η_1 and η_2 are two nonnegative weight constants.

3.1. Level Set Formulation

In level set method, contour $\mathcal{C}$ is represented by the zero level set of a Lipschitz function $\phi : \Omega \to \mathbb{R}$, which is called a level set function. The segmentation contour, foreground and background regions are represented by $\mathcal{C} = \{\mathbf{x} | \phi(\mathbf{x}) = 0\}$, $\Omega_f = \{\mathbf{x} | \phi(\mathbf{x}) > 0\}$ and $\Omega_b = \{\mathbf{x} | \phi(\mathbf{x}) < 0\}$, respectively. The final objective function is

$$\begin{aligned} \mathcal{F}_{eo}(\phi, C_f, C_b) = \mathcal{F}_{lbf}(\phi, C_f, C_b) + \nu \mathcal{L}(\phi) + \mu \mathcal{P}(\phi) \\ + \eta_1 \mathcal{F}_{op}(C_f, C_b) + \eta_2 \mathcal{F}_{os}(C_f, C_b), \end{aligned} \tag{10}$$

where μ and ν are the weighting constants. $\mathcal{L}(\phi)$ is the contour length term, which is defined as:

$$\mathcal{L}(\phi) = \int_\Omega |\nabla H(\phi(\mathbf{x}))| \, d\mathbf{x}, \tag{11}$$

and $\mathcal{P}(\phi)$ is the regularization term proposed in [18], which is defined as

$$\mathcal{P}(\phi) = \int_\Omega \frac{1}{2} (|\nabla \phi(\mathbf{x})| - 1)^2 \, d\mathbf{x}. \tag{12}$$

When implementation, the Heaviside function $H(.)$ is approximated by the ϵ-Heaviside function

$$H_\epsilon(x) = \frac{1}{2}\left[1 + \frac{2}{\pi} \arctan\left(\frac{x}{\epsilon}\right)\right], \tag{13}$$

and the corresponding derivation is defined by

$$\delta_\epsilon(x) = H'_\epsilon(x) = \frac{\epsilon}{\pi(\epsilon^2 + x^2)}. \tag{14}$$

In our implementation, parameter ϵ is set to 1.0.

3.2. Semi-Implicit Optimization

Same with LBF model, the standard gradient descent method is utilized to minimize the energy functional Eqn. (10).

Step 1: For a fixed level set function ϕ, we minimize the energy functional $\mathcal{F}_{eo}$ with respect to C_f and C_b using the standard gradient descent method by solving the gradient flow equation as follows:

$$\frac{dC_f}{dt} = -\frac{\partial \mathcal{F}_{eo}}{\partial C_f} = A_1 C_f - [b_1 + 2\eta_1 \cdot h_1 + 4\eta_2 \cdot (h_1 - h_2)], \tag{15}$$

where

$$\begin{aligned} A_1 &= -2\lambda_f (K_\sigma \otimes H_\epsilon(\phi)), \\ b_1 &= -2\lambda_f (K_\sigma \otimes (H_\epsilon(\phi) \odot I)), \\ h_1 &= H_\epsilon(C_f - C_b)\delta_\epsilon(C_f - C_b) \int B(\mathbf{x}, \mathbf{y}) d\mathbf{y}, \\ h_2 &= \delta_\epsilon(C_f - C_b) \int B(\mathbf{x}, \mathbf{y}) H_\epsilon(C_f - C_b) d\mathbf{y}, \end{aligned}$$

in which $\otimes$ is the convolution operation and $\odot$ is Hadamard product. Therefore, Eqn. (15) can be rewritten as

$$\frac{C_f^{t+1} - C_f^t}{\Delta t} = A_1 C_f^t - (b_1 + 2\eta_1 h_1^t + 4\eta_2 (h_1^t - h_2^t)). \tag{16}$$

Under semi-implicit implementation, Eqn. (16) is reformulated as

$$\frac{C_f^{t+1} - C_f^t}{\Delta t} = A_1 C_f^{t+1} - (b_1 + 2\eta_1 h_1^t + 4\eta_2 (h_1^t - h_2^t)). \tag{17}$$

Then, we have

$$C_f^{t+1} = \frac{C_f^t - (b_1 + 2\eta_1 \cdot h_1^t + 4\eta_2 \cdot (h_1^t - h_2^t))\Delta t}{I - A_1 \Delta t} \quad (18)$$

Similarly, for C_b, we have

$$C_b^{t+1} = \frac{C_b^t - \left(b_2 - 2\eta_1 \cdot h_1^t - 4\eta_2 \cdot \left(h_1^t - h_2^t\right)\right)\Delta t}{I - A_2 \Delta t} \quad (19)$$

where

$$\begin{aligned} A_2 &= -2\lambda_1 (K_\sigma \otimes (1 - H_\epsilon(\phi))), \\ b_2 &= -2\lambda_1 (K_\sigma \otimes ((1 - H_\epsilon(\phi)) \odot I)). \end{aligned}$$

Step 2: Keeping C_f and C_b fixed, we minimize the energy functional $\mathcal{F}_{eo}$ with respect to ϕ using the standard gradient descent method by solving the gradient flow equation as follows:

$$\begin{aligned} \frac{\partial \phi}{\partial t} = &-\delta_\varepsilon(\phi)(\lambda_1 e_1 - \lambda_2 e_2) + \nu \delta_\varepsilon(\phi) \operatorname{div}\left(\frac{\nabla \phi}{|\nabla \phi|}\right) \\ &+ \mu\left(\nabla^2 \phi - \operatorname{div}\left(\frac{\nabla \phi}{|\nabla \phi|}\right)\right), \end{aligned} \quad (20)$$

where

$$e_i(\mathbf{x}) = \int K_\sigma(\mathbf{y} - \mathbf{x}) |I(\mathbf{x}) - f_i(\mathbf{y})|^2 d\mathbf{y}, \quad i = 1, 2. \quad (21)$$

The **Step 2** is same with the LBF model.

3.3. Implementation Details

In Eqn. (22), the partial derivative is simply discretized as the central finite difference, and the temporal derivative is discretized as a forward difference. The Gaussian kernel K_σ is truncated as an $m \times m$ mask, where $m = 4\sigma + 1$ and $\sigma = 3$. The main procedures of our method is summarized as follows:

STEP_1. Initialize the level set function ϕ^0 by Eqn. (22):

$$\phi^0 = \phi(\mathbf{x}, t = 0) = \begin{cases} -\rho & \mathbf{x} \in \Omega_f - \partial\Omega_f \\ 0 & \mathbf{x} \in \partial\Omega_f \\ \rho & \mathbf{x} \in \Omega - \Omega_f \end{cases}, \quad (22)$$

where $\partial\Omega_f$ is the boundary of Ω_f.

STEP_2. Evolve C_f and C_b by Eqns. (18) and (19).

STEP_3. Evolve the level set function ϕ according to Eqn. (23). To obtain the numeric solution of Eqn. (23), the current level set ϕ^{n+1} is updated by the previous iteration result ϕ^n, given by

$$\phi^{n+1} = \phi^n + \Delta t \frac{\partial \phi^n}{\partial t}, \quad (23)$$

where Δt is the time-step.

STEP_4. Repeat **STEP_2** and **STEP_3** until ϕ is converged or the maximum iteration number is reached.

4. EXPERIMENTAL RESULTS

A number of images are used to evaluate our method by comparing with two global region-based methods, i.e., CV [7] [1], TVCV [19] [2], and two local-region based methods, i.e., LIF [13] [3], LBF [12] [4].

[1]The codes are available at www.mathworks.com/matlabcentral/fileexchange/23445.

[2]The codes are available at www.cs.cityu.edu.hk/~xbresson/codes.html.

[3]The codes are available at www4.comp.polyu.edu.hk/~cskhzhang/.

[4]The codes are available at www.engr.uconn.edu/~cmli/.

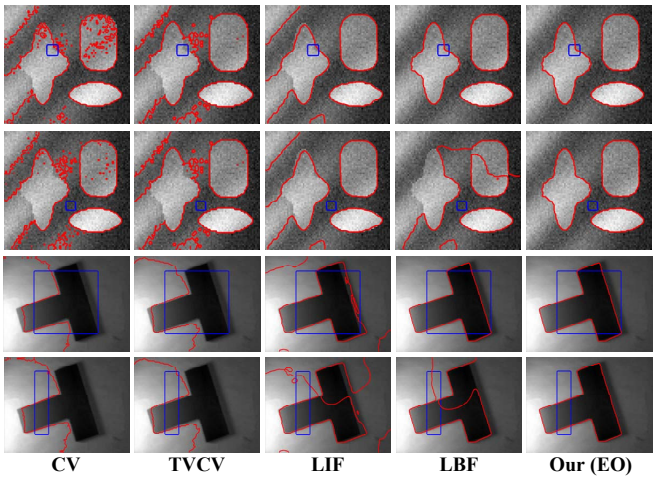

Fig. 1. Comparative results of the proposed method with CV, TVCV, LIF, and LBF on two synthetic images. The initial and final contours are in blue and red, respectively.

4.1. Comparisons On Synthetic Images

In the first experiment, we compare our method with the state-of-the-art approaches on two synthetic images, and the results are shown in Fig. 1. As shown in this figure, two global-region based methods and LIF cannot segment the objects out. As shown in the third and fourth columns, two local-region based methods, i.e., LIF and LBF are both sensitive to initializations. Moreover, the results of LIF cannot fit real object edges. By contrast, our method not only segments out the objects, but also is very stable to initial contours.

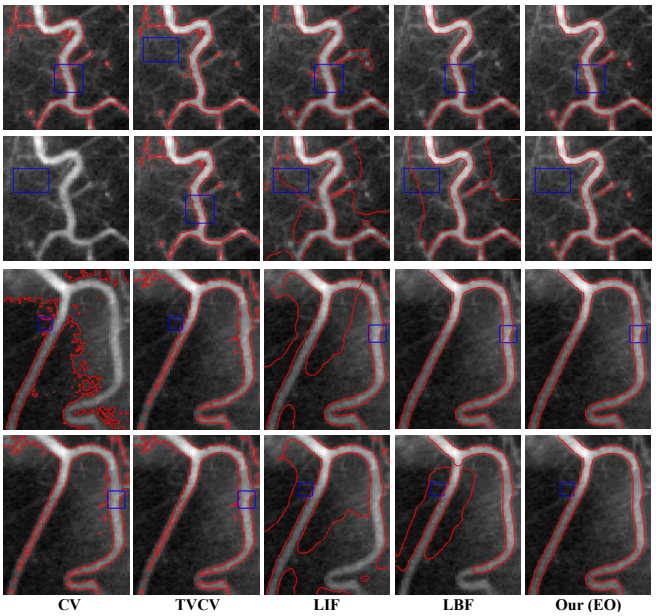

Fig. 2. Comparative results of the proposed method with CV, TVCV, LIF, and LBF on two blood vessel images. The initial and final contours are in blue and red, respectively.

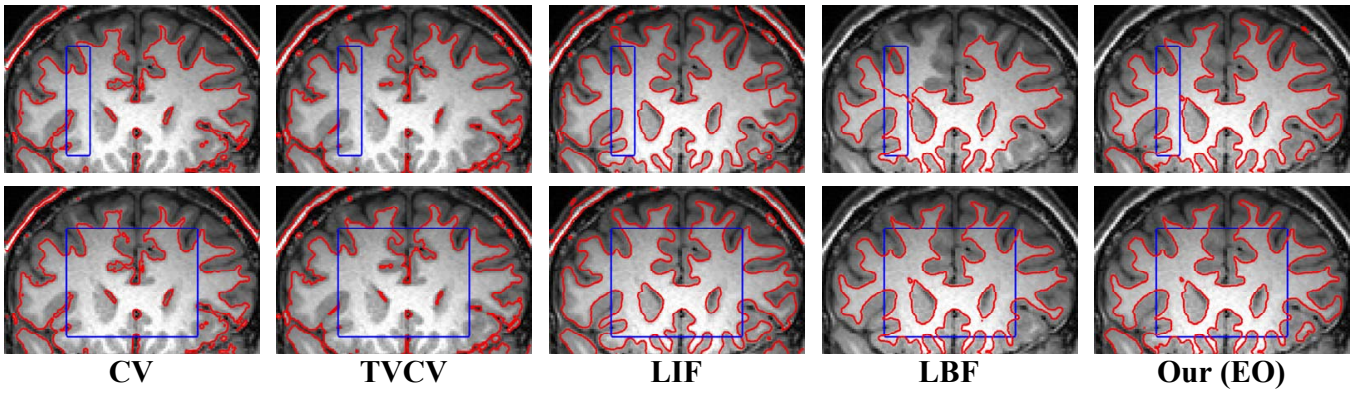

Fig. 3. Comparative results of the proposed method with CV, TVCV, LIF, and LBF on MR image. The initial and final contours are in blue and red, respectively.

4.2. Comparisons On Real Images

In the second experiment, we compare our method with the state-of-the-art approaches on real images. Fig. 2 presents two comparisons on blood vessel images. Except intensity inhomogeneous, the main difficulty on blood vessel image is that the object is vimineous. Fig. 3 gives one comparison on MR image, in which the intensity inhomogeneity is caused by the instability of magnetic field. Hence, in MR image, the intensity inhomogeneous problem is particularly serious. Same with the results on synthetic images, our method obtains more excellent segmentation results than the others.

4.3. Noise Sensitivity

We also evaluate the noise sensitivity of our method on two synthetic images. The noise images are simulated by adding Gaussian noise on the input images. Here, we utilize the function of 'imnoise' in Matlab to generate noise images. We select six noise levels, i.e., $10^{-3}, 2\times10^{-3}, 5\times10^{-3}, 10^{-2}, 2\times10^{-2}, 5\times10^{-2}$. The segmentation results are shown in Fig. 4. From this figure, we see that our algorithm still can segment out these objects on the whole, although the images are distorted by noises.

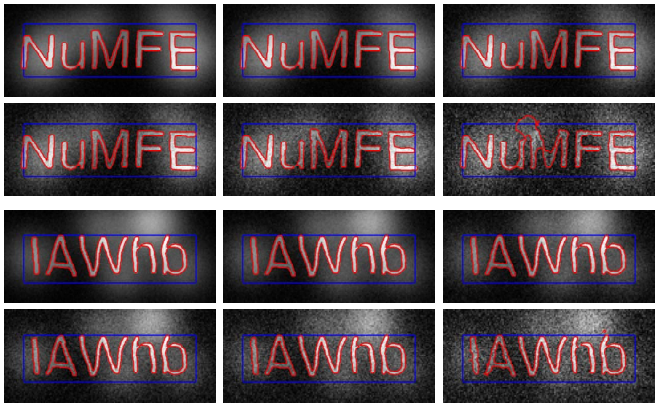

Fig. 4. Segmentation results on two synthetic images of our method with six different noise levels, such as $10^{-3}, 2\times10^{-3}, 5\times10^{-3}, 10^{-2}, 2\times10^{-2}, 5\times10^{-2}$ (from left to right and from top to bottom).

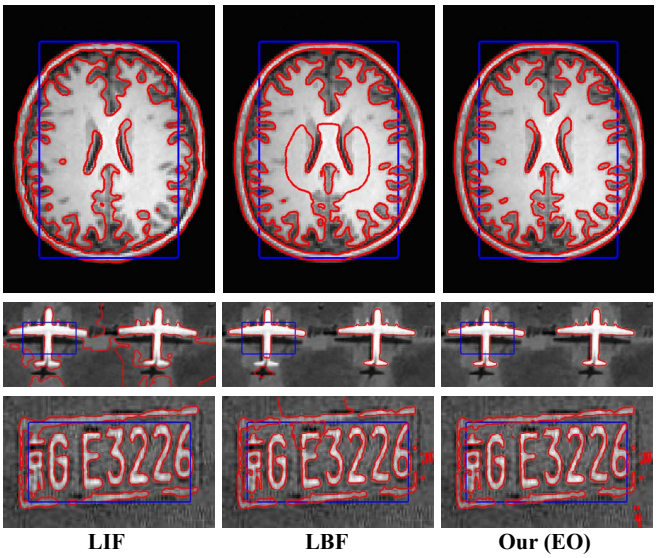

Fig. 5. More comparative results with two local-region based methods, i.e., LIF, and LBF.

4.4. More Results

We select three images with different image types, including medical image, remote sensing image and natural image, to evaluate our method. The segmentation results are illustrated in Fig. 5. From this figure, we can see that our results are better than those of LIF and LBF in a whole. These results can further demonstrate the effectiveness of our algorithm.

5. CONCLUSION

In this paper, we propose two explicit order models, i.e., the GOP and LOS models, to remedy the initialization sensitive problem of the LBF model in image segmentation. Experiments on several challenge synthetic and real images show that our method is less sensitive to initialization as compared with LBF. However, our method still has some limitations. For example, our method is hard to be applied to the segmentation of wispy targets, such as capillaries.

6. REFERENCES

[1] Michael Kass, Andrew Witkin, and Demetri Terzopoulos, "Snakes: Active contour models," *International Journal of Computer Vision*, vol. 1, no. 4, pp. 321–331, 1988.

[2] Vicent Caselles, Ron Kimmel, and Guillermo Sapiro, "Geodesic active contours," *IEEE International Conference on Computer Vision*, pp. 694–699, 1995.

[3] Vicent Caselles, Ron Kimmel, and Guillermo Sapiro, "Geodesic active contours," *International Journal of Computer Vision*, vol. 22, no. 1, pp. 61–79, 1997.

[4] Chenyang Xu and Jerry L. Prince, "Snakes, shapes, and gradient vector flow," *IEEE Transactions on Image Processing*, vol. 7, no. 3, pp. 359–369, 1998.

[5] Nikos Paragios and Rachid Deriche, "Geodesic active contours and level sets for the detection and tracking of moving objects," *IEEE Transactions on Pattern Analysis and Machine Intelligence*, vol. 22, no. 3, pp. 266–280, 2000.

[6] Nikos Paragios and Rachid Deriche, "Geodesic active regions and level set methods for supervised texture segmentation," *International Journal of Computer Vision*, vol. 46, pp. 223–247, 2002.

[7] Tony F. Chan and Luminita A. Vese, "Active contours without edges," *IEEE Transactions on Image Processing*, vol. 10, pp. 266–277, 2001.

[8] Luminita A. Vese and Tony F. Chan, "A multiphase level set framework for image segmentation using the mumford and shah model," *International Journal of Computer Vision*, vol. 50, pp. 271–293, 2002.

[9] Mila Nikolova, Selim Esedoglu, and Tony F. Chan, "Algorithms for finding global minimizers of image segmentation and denoising models," *SIAM Journal of Applied Mathematics*, vol. 66, no. 5, pp. 1632–1648, 2006.

[10] D. Cremers, S.J. Osher, and S. Soatto, "Kernel density estimation and intrinsic alignment for shape priors in level set segmentation," *International Journal of Computer Vision*, vol. 69, no. 3, pp. 335–351, 2006.

[11] Daniel Cremers, "Nonlinear dynamical shape priors for level set segmentation," *Journal of Scientific Computing*, vol. 35, no. 2-3, pp. 132–143, 2008.

[12] Chunming Li, Chiu-Yen Kao, John C. Gore, and Zhaohua Ding, "Minimization of region-scalable fitting energy for image segmentation," *IEEE Transactions on Image Processing*, vol. 17, no. 10, pp. 1940–1949, 2008.

[13] K.H.Zhang, H.H.Song, and Lei Zhang, "Active contours driven by local image fitting energy," *Pattern Recognition*, vol. 43, no. 4, pp. 1199–1206, 2010.

[14] Shigang Liu and Yali Peng, "A local region-based chan-vese model for image segmentation," *Pattern Recognition*, vol. 45, no. 7, pp. 2769–2779, 2012.

[15] LingFeng Wang, Zeyun Yu, and Chunhong Pan, "A unified level set framework utilizing parameter priors for medical image segmentation," *Science China Information Sciences*, vol. 55, pp. 1–14, 2012.

[16] LingFeng Wang, Huai-Yu Wu, and Chunhong Pan, "Region-based image segmentation with local signed difference energy," *Pattern Recognition Letters*, vol. 34, no. 6, pp. 637–645, 2013.

[17] Y.Y. Boykov and M.-P. Jolly, "Interactive graph cuts for optimal boundary and region segmentation of objects in n-d images," *International Conference on Computer Vision*, vol. 1, no. 10, pp. 105–112, 2001.

[18] Chunming Li, Chenyang Xu, Changfeng Gui, and Martin D. Fox, "Level set evolution without re-initialization: A new variational formulation," in *IEEE Conference on Computer Vision and Pattern Recognition*, 2005, pp. 430–436.

[19] Tom Goldstein, Xavier Bresson, and Stanley Osher, "Geometric applications of the split bregman method: Segmentation and surface reconstruction," *Journal of Scientific Computing*, vol. 45, no. 1-3, pp. 272–293, 2010.